Characterization of leaf–level particulate matter for an industrial city using electron microscopy and X-ray microanalysis

Sgrigna G.[1,2]; Baldacchini C.[2]; Esposito R.[2]; Calandrelli R.[2]; Tiwary A.[3]; Calfapietra C.[2,4,*]

[1]University of Molise (UniMol), Department of Biosciences and Territory – Contrada Fonte Lappone Pesche (IS), Italy – e-mail: gregorio.sgrigna@ibaf.cnr.it

[2]Institute of Agro Environmental and Forest Biology, National Research Council (IBAF – CNR) – Via Marconi, 2 Porano (TR) & Via Castellino 111, Napoli, Italy – e-mail: chiara.baldacchini@ibaf.cnr.it; raffaela.esposito@ibaf.cnr.it; roberto.calandrelli@ibaf.cnr.it; carlo.calfapietra@ibaf.cnr.it

[3]Faculty of Engineering and the Environment, University of Southampton, Highfield Campus, Southampton SO17 1BJ, U.K. - e-mail: a.tiwary@soton.ac.uk

[4]Global Change Research Centre, Academy of Sciences of the Czech Republic, v. v. i., Bělidla 986/4a, 603 00 Brno, Czech Republic

Abstract

This study reports application of monitoring and characterization protocol for particulate matter (PM) deposited on tree leaves, using *Quercus ilex* as a case study species. The study area is located in the industrial city of Terni in central Italy, with high PM concentrations. Four trees were selected as representative of distinct pollution environments based on their proximity to a steel factory and a street. Wash off from leaves onto cellulose filters were characterized using scanning electron microscopy and energy dispersive X-ray spectroscopy, inferring the associations between particle sizes, chemical composition, and sampling location. Modeling of particle size distributions showed a tri-modal fingerprint, with the three modes centered at 0.6 (factory related), 1.2 (urban background), and 2.6 μm (traffic related). Chemical detection identified 23 elements abundant in the PM samples. Principal component analysis recognized iron and copper as source-specific PM markers, attributed mainly to industrial and heavy traffic pollution respectively. Upscaling these results on leaf area basis provided a useful indicator for strategic evaluation of harmful PM pollutants using tree leaves.

Keywords: *Air pollution; EDX; Human health; Particulate matter; SEM; Urban trees*

1. Introduction

For over a decade, Particulate matter (PM) has remained the focus of longitudinal studies associating ambient pollution exposure with potential human health effects (Dai et al., 2014; Cheng et al., 2013; Anderson et al., 2012; Dockery et al., 1993; Kumar et al., 2011; Samet et al., 2000). Several sampling and analysis methodologies have evaluated the quality of urban PM for a range of environments, including traffic (Pant and Harrison, 2013; Grigoratos and Martini, 2015), indoor metro stations (Lu et al., 2015; Querol et al., 2012), industries (Deshmukh et al., 2012), and the wider suburbs (Blanco et al., 2003). Human health is shown to be affected more by enhanced exposure levels to cumulative PM (mainly associated with pulmonary diseases) or their chemical composition (Donaldson and Seaton, 2012; Warheit et al., 2007) than by single events of acute pollutant concentration (Kariisa et al., 2014). For instance, exacerbated exposure to iron (Fe) particles has been suggested to directly affect human cell permeability (Apopa et al., 2009).

Trees have been found effective in PM removal in cities (Escobedo et al., 2011; McDonald et al., 2007; Tiwary et al., 2009). This has led to new urban tree planting programs, prioritizing tree species selection with greater pollution mitigation potential, alongside choosing strategic locations for their optimal outcomes (Calfapietra et al., 2013; Llausàs and Roe, 2012; Morani et al., 2011). Unlike other gaseous pollutants which are mainly removed via stomatal flux, gravitational and/or inertial deposition on lamina and tips have been considered the main PM removal mechanisms for leaves (Beckett et al., 1998; Hofman et al., 2014a; Popek et al., 2013; Tiwary et al., 2006; Tomašević et al., 2005).

The influence of leaf shape and morphology on PM deposition has also been extensively studied (Dzierzanowski et al., 2011; Freer-Smith et al., 2005; Popek et al., 2013; Song et al., 2015). The canopy-scale PM reduction potentials have been assessed through measurement campaigns (Jin et al., 2014; Peachey et al., 2009) as well as through empirical modeling approaches (Nowak et al., 2008), elucidating the role of the morphological (e.g. canopy structure, tree assemblage, leaf dimension, etc.) and the locational characteristics of urban trees in PM removal. Moreover, it is noteworthy that a large PM deposition on leaves can alter leaf physiology, thereby further influencing the air pollution mitigation potential of trees (Calfapietra et al., 2015).

This study reports the development of a monitoring and characterization protocol for leaf-level PM deposits in urban environments. Leaves of trees, located at strategic points within the study area, have been used as natural passive PM samplers to determine the associations between particle size, chemical composition, and their locational influences (if any). The first part describes the methodology adopted, specifcially elaborating on the customization of the sampling and analysis techniques to estimate the leaf-level PM quality. This is followed by its implementation to a case study and a brief description of the obtained results. The study concludes with a discussion on the application potentials of the proposed leaf analysis approach as a useful indicator for strategic evaluation of human exposure to harmful PM pollutants on a routine basis, typically applicable to industrial cities.

2. Materials and Methods

2.1 Study Area

The study area is the industrial city of Terni, located in the Umbria region of central Italy with approximately 112,000 inhabitants. This site has been chosen as it is the most industrialized city in the region, characterized by high average levels of PM_{10} concentration in the air (Sgrigna et al., 2015) (www.arpa.umbria.it). Three industrial hubs are included in the Terni urban area (Capelli et al., 2011), among which the "Thyssen Krupp AST" (*Acciai Speciali Terni* – Special Steels Terni) steel factory is located in the eastern part of the city, occupying an area of approximately 158 ha. The city is located in a valley, surrounded by two main mountain chains together with a smaller one (Cattuto et al., 2002). Apparently, the presence of industrial hubs and urban activities within the valley has been contributing to several recorded exceedances of PM concentration throughout the year, particularly over stable atmospheric conditions during the winter and the summer months (www.arpa.umbria.it).

2.2. Sampling and filtering

Leaf samples were collected from four trees of *Quercus ilex* (holm oak, approximately 10 m high) on 23 August 2012. The trees were located in two different parts of Terni, and were considered as representative of the distinct site characteristics in terms of their proximity to a street and/or to the steel factory. Figure 1 provides a spatial reference to this site, along with a wind rose of the study area, specifically depicting the areas considered as far from and close to the steel factory (FF, spot 1, and CF, spot 2, respectively). The effect of the steel factory on trees was established from peak PM deposition, in consistency with the local environmental control stations, estimated on the basis of the height of the industrial stacks and the prevailing winds (Sgrigna et al., 2015; Tadmor, 1971). For each study location, two sampling trees were selected at different distances from a traffic PM source, far from other pollutant sources: one on the side of a street with an average traffic between 330 and 430 vehicles h^{-1} (street tree, S) and the other in a park at a distance of about 25 m from streets and surrounded by other trees (park tree, P). The four sampled trees were identified by the following codes and coordinates: FFP (42°34'46.69'' N, 12°37'31.19'' E); FFS (42°34'47.26'' N, 12°37'31.55'' E); CFP (42°33'05.75'' N, 12°38'53.09'' E); and CFS (42°33'14.58'' N, 12°38'56.29'' E).

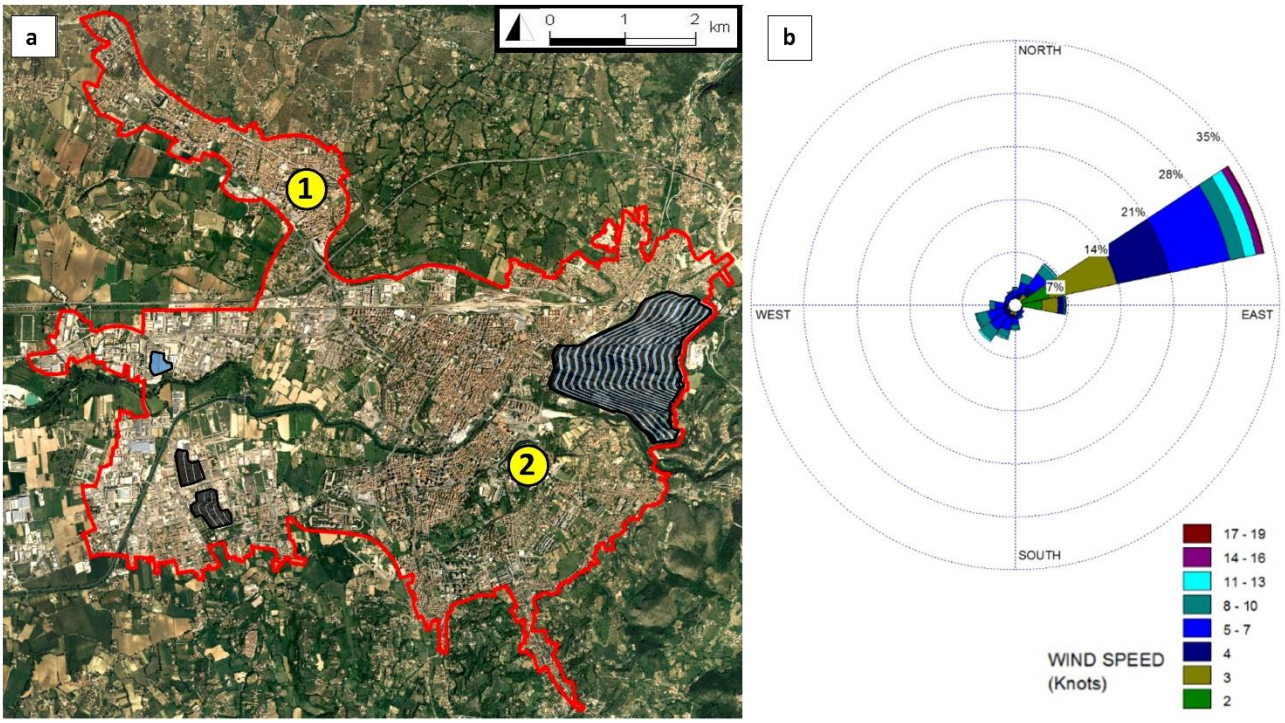

Figure 1 – (a) Geo-referenced map showing the sampling areas (FF and CF respectively highlighted as 1 and 2), the steel factory area within the city borders (striped area on the eastern side), the chemical pole (gray areas in the south-western side), and the waste treatment area (north-western side); (b) wind rose showing the prevailing wind in the study area (annual average, 2012).

Approximately between 300 and 500 cm^2 of leaf area was sampled for each sampling tree, at two sampling heights (8 and 2 m). Leaves from street trees were gathered from the street-facing sides. Sampled leaf material was separately washed in micro-distilled water, followed by filtration using quantitative filter papers according to the standard protocols (Dzierzanowski et al., 2011; Freer-Smith et al., 2005; Sgrigna et al., 2015). First, PM > 10 µm were removed from the wash off using filters with porosity between 10 and 13 µm (Anoia S.A., Barcelona, code 1250). Then, coarse and fine PM 2.5 were collected on filter papers with porosity between 2 and 4 µm (Anoia S.A. Barcelona, code: 1244); such filters were then used for PM characterization.

2.3 Scanning Electron Microscopy and Energy-Dispersive X-ray spectroscopy analyses

Particle size and elemental composition of PM fixed on cellulose filters were obtained through scanning electron microscopy (SEM) and energy-dispersive X-ray spectroscopy (EDX) analysis, respectively. These data allowed us to estimate the total collected volume of the different elements on sampled leaves and the corresponding upscale on the leaf area basis. Previous studies have applied SEM/EDX analysis for *in situ* PM monitoring on the leaves of trees and shrubs (Lorenzini et al., 2006; Lu et al., 2008; Sawidis et al., 2011; Simon et al., 2014; Tomašević et al., 2005), usually associated with atomic absorption measurements. However, our methodology focused on quantifying the insoluble part of PM, by washing the leaves (Dzierzanowski et al., 2011; Freer-Smith et al., 2005; Sgrigna et al., 2015) and analyzing the residue of the wash off on cellulose filter. This procedure enabled selection of the most persistent particles, which often tend to be accumulated on the majority of exposed surfaces, including human epithelial tissues (Anderson et al., 2012).

SEM/EDX analyses were performed on filter pairs from each sampling height. Two fragments of area 1 cm^2 were cut from each filter, one at the center and the other at the border, and analyzed. A Phenom ProX microscope (Phenom-World BV®, The Netherlands, 2014) with dedicated Phenom Pro Suite software was used. Imaging and elemental data were acquired at an incident electron energy of 15 KeV.

Random images with a scan size of 30 × 30 µm were acquired, at a resolution of 1024 × 1024 pixels. A representative image is shown in Figure 2a. Approximately 200 particles were randomly selected per filter (100 per fragment), totaling to 3129 particles altogether (about 400 particles at each of the two heights, for the four trees). For every particle, the diameter of the equivalent sphere (d_{eq}) was obtained by averaging the two main Feret diameters (Merkus, 2009), as measured by ImageJ open source software (Rasband, W.S., ImageJ, U. S. National Institutes of Health, Bethesda, Maryland, USA, 1997-2014). On the basis of the chosen imaging conditions (30-µm scan size, at a resolution of 1024 × 1024 pixels), particles with d_{eq} < 100 nm (i.e. effective width < 3 pixels) were excluded from the analyses.

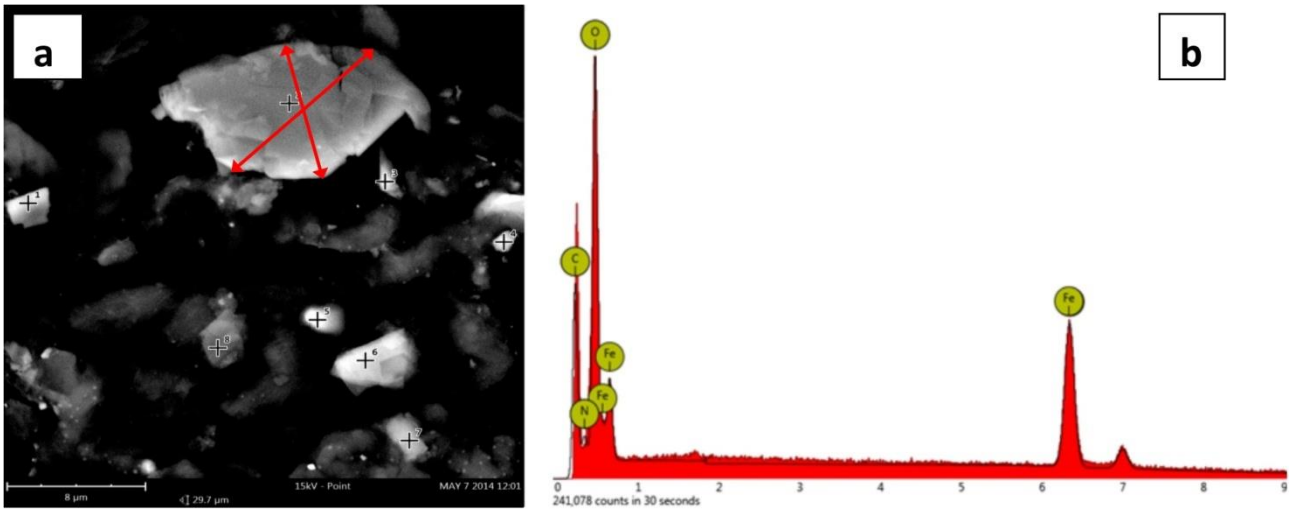

Figure 2 - (a) Representative SEM image showing PM on a paper filter fragment; the two main Feret diameters of the largest particle are marked by red arrows; the laser beam position during the acquisition of the EDX spectra from the selected particles is indicated by black crosses; (b) representative EDX spectrum of an iron-containing particle.

Particle d_{eq} distributions were assumed to follow a lognormal behavior, as expected for particles grown under Brownian coagulation (Lee and Chen, 1984), condensation (Söderlund et al., 1998), or nucleation (Ackermann et al., 1998). Lognormal functions are generally used to describe aerosol particle dimensions (William C. Hinds, 1999), and also in specific cases such as marine aerosol (Smith et al., 1993) or biomass burning aerosol emissions from vegetation fires (Janhäll et al., 2009). Multi-modal lognormal fitting was performed using OriginPro 8.5 software (OriginLab®, Northampton, MA, USA), and each mode was described following Equation 1.

$$f(x)_{X,\sigma} = A\ \frac{-\frac{(lnx-lnX)^2}{2\sigma^2}}{x\sqrt{2\pi}\,\sigma} \qquad (1)$$

where, *A* represents the abundance of each mode in terms of relative frequencies; *X* is the mean diameter; and σ is the standard deviation. Models with different number of modes were compared based on the adjusted r^2 and reduced χ^2 values, as obtained by the analysis software; the number of modes being increased until adjusted $r^2 > 0.95$ and reduced $\chi^2 < 0.5$ were obtained.

EDX spectra for the elemental analysis were obtained by positioning the laser beam in the center of randomly selected particles (black cross markers in Figure 2a). A representative EDX spectrum is shown in Figure 2b. The main elements identified in the particles were C, N, O, F, Na, Mg, Al, Si, P, S, Cl, K, Ca, Ti, Cr, Mn, Fe, Ni, Cu, Zn, Mo, Sn, Sb, Ba, W, and Bi. Particles showing only C, N, and O were excluded from the analysis, because of the uncertainty of EDX in quantifying those lighter elements and the difficulties introduced by the use of cellulose filters as substrates (Wilkinson et al., 2013).

A semi-quantitative estimation of the elemental composition was obtained by calculating the weighted volume percentage ($W_{\%}$) occupied by each element *x* over the N selected particles. This was obtained as a product of the composition C (as percentage) of each element x on each particle i (C_{xi}, as obtained by the EDX software) and the corresponding particle volume V_i, as obtained by the diameter of the equivalent sphere d_{eq} ($V_i = 4/3\ \pi\ (d_{eq}/2)^3$). Then, for each element *x* these volumes were summed together, and the sum was

normalized by using the total analyzed particle volume. The resulting $W_{\%}$ for each element *x* was obtained following Equation 2.

$$W_{\%_x} = \frac{\sum_{i=1}^{N} C_{x_i} \times V_i}{\sum_{i=1}^{N} V_i} \qquad (2)$$

2.4 Principal Components Analysis

The elemental composition of PM obtained for the different sites was further analyzed through principal component analysis (PCA), as a statistical multivariate approach using Statistica 7.0 software (StatSoft Inc. USA, 2004). The results of the PCA based on covariance were applied to the EDX data set, allowing interpretation of the site differences (as weighted percentages) and relationships between detected elements and the sampled tree locations.

The variables considered for the PCA were the values of $W_{\%}$ of those elements which were recorded at all sites as >0.2% (i.e. F, Na, Mg, Al, Si, P, S, Cl, K, Ca, Ti, Fe, and Cu). The remaining low-concentrated 10 elements (Cr, Mn, Ni, Zn, Mo, Sn, Sb, Ba, W, and Bi) were treated as a single "residual" variable (Wilkinson et al., 2013). C, N, and O were excluded from the PCA for the reasons mentioned in Section 2.3. The selected 14 PCA variables were then normalized; the resulting PCA input matrix is reported in detail in the Supplementary Material (SM1).

3. Results

3.1 Particle size distribution

The measured particle equivalent diameters (d_{eq}) ranged between 0.1 and 10 µm, with up to 97% of the particles in the size range 0.1–5.0 µm. The average particle dimension for the entire sample was found to be 1.57 ± 0.06 µm. The mean d_{eq} measured at the four sampling sites were: 1.6 ± 1.4 µm (FFP), 1.7 ± 1.3 µm (FFS), 1.4 ± 1.4 µm (CFP), and 1.6 ± 1.3 µm (CFS); such values being not statistically different. The histograms

in Figure 3 show the distributions of the PM equivalent diameter (d_{eq}) at the four sites, considering the total particles collected for each tree. The curves resulting from the applied multi-modal lognormal fitting procedure are also shown alongside, and the corresponding parameters have been listed in Table 1.

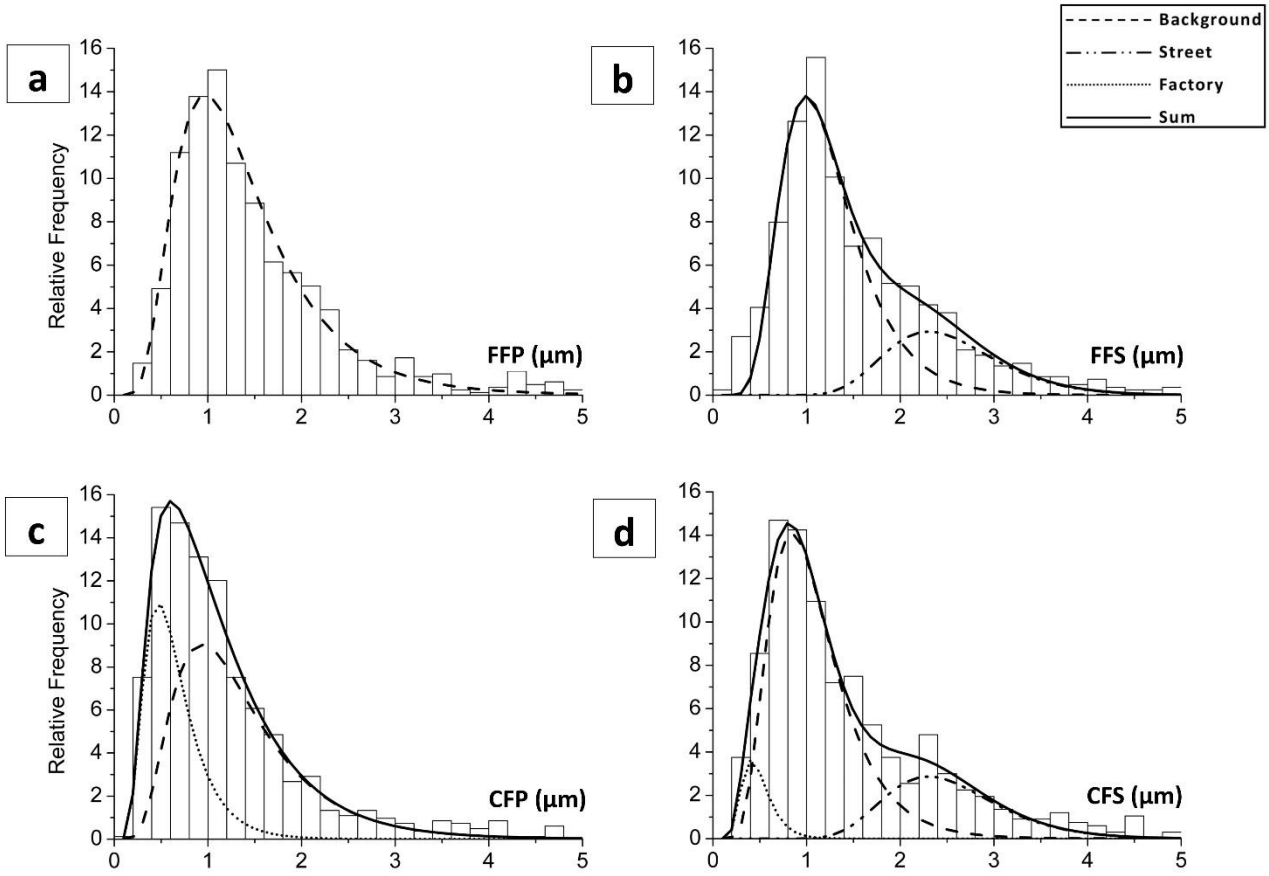

Figure 3 – Equivalent diameter (d_{eq}) distributions and their multimodal fitting, at the four sampling sites: (a) FFP – park site far from the factory; (b) FFS – street site far from the factory; (c) CFP – park site close to the factory; and (d) CFS – street site close to the factory. Dashed line: Background mode; dash-dot-dot line: Street mode; dotted line: Factory mode; solid line: sum of the modes.

The following key observations were made - park tree far from the factory (FFP) was considered as representative of the city background pollution signal: its d_{eq} distribution (Figure 3a) is well described by a single lognormal mode (labeled as "Background" in Table 1), which is centered at about 1.24 µm and has a standard deviation $\sigma = 0.49 \pm 0.01$ µm. On the contrary, the distribution of the particles collected far from the factory but close to the street (FFS) could not be adequately described by a single lognormal function, neither centered at 1.2 µm (fixed position) nor with free center position (which resulted to be at 1.3 µm), based on the adjusted r^2 and reduced χ^2 values. A suitable fitting function for this distribution was obtained

only after addition of a second mode centered at a higher d_{eq} with respect to the "Background" mode at 1.2 µm (Figure 3b). This additional mode (labeled as "Street" in Table 1) resulted to be centered at about 2.6 µm, with a standard deviation of 0.23 ± 0.05 µm. The spread for the "Background" mode d_{eq} distribution was found to be similar to that observed at the FFP site (σ = 0.41 ± 0.02 µm). Similarly, the d_{eq} distribution of the particles collected far from the street but close to the factory (CFP) required an additional mode to be adequately described as well. This additional mode (labeled as "Factory" in Table 1) resulted in a shift toward lower diameters with respect to the "Background" mode, being centered at about 0.58 µm, with a spread of σ = 0.46 ± 0.04 µm (Figure 3c). Finally, the d_{eq} distribution obtained from the tree close to both the street and the factory (CFS) is shown in Figure 3d. It was tentatively fitted by adding a single mode to the "Background" one, as done for the other two sites, with unsuccessful results. A good fitting curve was obtained only by imposing a tri-modal model. In particular, the fitting curve obtained by summing three lognormal functions centered at 0.6, 1.2, and 2.6 µm (fixed fitting parameters) is shown in Figure 3d. Notably, the resulting standard deviation of each mode (free fitting parameters) was in line with those obtained for the d_{eq} distributions at the other sites.

Table 1 – Multi-modal fitting parameters for equivalent diameter distribution (d_{eq}): mean diameter (X), standard deviation (σ), and relative abundance (A) for the three detected modes ("Factory," "Background," and "Street"). The statistical error value on the X parameter is missing for those modes whose position was kept fixed during the fitting procedure. The relative model statistics (adjusted R^2 and reduced χ^2) are reported for each fitting.

Mode	***Factor***	***Sampling site***			
		FFP	**FFS**	**CFP**	**CFS**
Factory	X	-	-	0.58 ± 0.03	0.6
	σ	-	-	0.46 ± 0.04	0.43 ± 0.05
	A	-	-	6.7 ± 0.4	1.3 ± 0.4
Background	X	1.24 ± 0.01	1.2	1.2	1.2
	σ	0.49 ± 0.01	0.41 ± 0.02	0.50 ± 0.03	0.51 ± 0.08
	A	18.9 ± 0.4	13.9 ± 0.6	12.1 ± 0.9	13.3 ± 0.4
Street	X	-	2.6 ± 0.1	-	2.6

	σ	-	0.23 ± 0.05	-	0.14 ± 0.06
	A	-	4.3 ± 0.8	-	4.3 ± 0.5
Adj-R ^{2}		0.98	0.97	0.99	0.98
Red-χ^2		0.22	0.42	0.15	0.28

Identical fitting procedures were applied at the d_{eq} distributions obtained by separately analyzing the particles collected in the lower and upper parts of the tree crown. The distributions corresponding to the same tree were well fitted by the same number of modes, centered at the same positions, but with a relative frequency ratio depending on the crown height. For instance, the d_{eq} distributions of particles collected far from the factory but close to the street (FFS) at different crown heights are shown in Figure 4, and it is evident that the "Street" mode is much intense at the lower sampling height. The relative abundances *A* of the three modes, as obtained by separately fitting the d_{eq} distributions of particles collected at the aforementioned two sampling heights, are presented in Table 2.

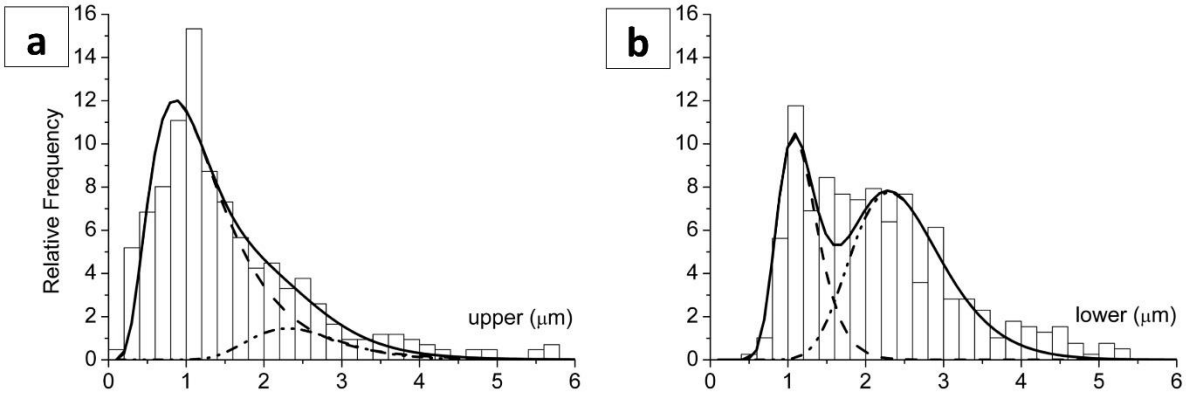

Figure 4 – Equivalent diameter (d_{eq}) distributions and the corresponding multi-modal fitted curves for particles detected at the FFS sampling site: (a) upper part of the tree crown; (b) lower part of the tree crown. Dashed line: "Background" mode; dash-dot-dot line: "Street" mode; solid line: sum of the modes.

Table 2 – Relative abundance (A) for the "Street" and "Factory" modes as obtained by lognormal multi-modal fitting of the d_{eq} distributions of particles separately collected at the upper (8 m) and lower (2 m) parts of the crown for the FFS, CFP, and CFS sites.

Mode	***Peak***	**Particle Abundance**					
		FFS-Up	**FFS-Low**	**CFP-Up**	**CFP-Low**	**CFS-Up**	**CFS-Low**
Street	X = 2.6 µm	1.0 ± 0.6	13.4 ± 0.8	-	-	1.0 ± 0.7	4.2 ± 1.7
Factory	X = 0.6 µm	-	-	7.3 ± 0.7	5.9 ± 0.3	6 ± 1	1.6 ± 0.9
Background	X = 1.2 µm	15.9 ± 0.8	6.8 ± 0.5	12.9 ± 0.5	15.3 ± 0.6	12.6 ± 0.4	12.1 ± 0.5

The abundance of larger particles was more prominent in the lower part of the crown for PM collected close to the street, both far (FFS) and close (CFS) to the factory. On the contrary, negligible vertical profiling in the PM population of fine particles for PM collected close to the factory were found, both at the park (CFP) and the street (CFS) sites. A minor relative abundance was obtained only in the lower part of the tree crown close to both the factory and street (CFS-Low), likely due to the significant relative intensity of the "Street" mode particles. It is noteworthy that the histogram areas were normalized, and the relative abundances do not represent the number of particles belonging to the specific mode, but their relative frequency. This explains the differences observed in the relative abundance of the "Background" mode among the different sites.

3.2 EDX analysis

The weighted volume percentages ($W_{\%}$) of the selected elements in the PM samples are shown in Figure 5. They represent the 29.0 ± 0.3% of the total particle volume detected (i.e. 29.2% at FFP, 30.0% at FFS, 28.5% at CFP, and 28.7% at CFS). The highest concentrations were observed for the "natural elements" (Na, Al, Si, K, Ca, and Fe), which can be attributed to the "crustal component" aerosol group (Amato et al., 2009; Lorenzini et al., 2006) or the "soil dust" component (Paoletti et al., 2003), and thus they are generally classified as "city dust" (Viana et al., 2008).

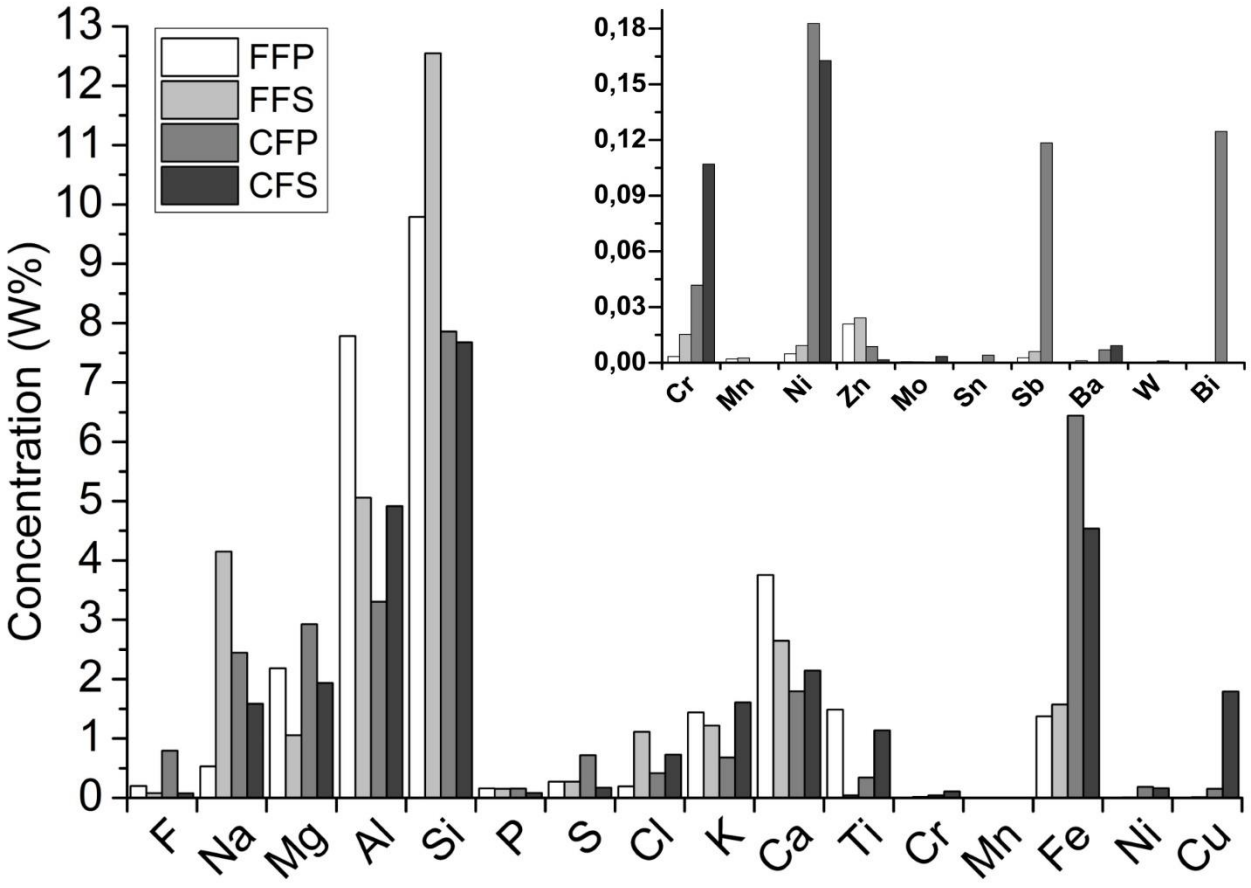

Figure 5 – Weighted volume percentages ($W_{\%}$) of the major elements and the trace elements (inset) obtained from EDX analyses. $W_{\%}$ measured at the different sites are shown on a gray scale (white - black), respectively representing FFP, FFS, CFP and CFS.

Significant differences in the metal concentrations for Fe, Cr, Ni, Sb, Ba, and Bi were observed in all areas, but their concentrations were at least three-fold at the site close to the factory (CF) than those far from it (FF). In particular, the Fe concentrations at the CFP and CFS sites were even higher than that of Na, K, and Ca. Trace metal elements, such as Mo, Sn, and W (Figure 5, inset) were observed only on samples close to the factory. Notably, both Cr and Cu were recorded at higher concentrations close to the streets (at both CFS and FFS). It is worth noting that Ti concentration showed a rather erratic pattern – the sites FFP and CFS

showed comparable concentrations, while only trace amounts were detected at both CFP and FFS sites; no correlation with the main sources considered in this study could be inferred.

3.3 Principal Components Analysis

Three principal components (PCs) were obtained from PCA. The PC projection on original variables, eigenvalues, and explained variance have been shown in the Supplementary Material (SM2). A clear distinction of the four sites (cases) was obtained by plotting their factor scores in the bi-dimensional plane, defined by PC1 and PC3 (Figure 6a). The horizontal axis is described by the most powerful component (PC1), which separates the sites close to the factory (CF sites, left-hand side of the plot) from those far from it (FF, right-hand side of the plot). The variable on the vertical axis of the plot in Figure 6a is PC3, which separates park (P, lower part of the plot) from street (S, upper part of the plot) sites.

The modeled representation was interpreted through the PC loadings, showing the driver elements for the considered factors and their relative weights. As shown by the variable loadings in Figure 6b, PC1 is distinguished between sampling sites characterized by Fe abundance (CFP and CFS), and the sites were dominated by the presence of Si, Al, and Ca (FFP and FFS). PC3 loadings indicated that the street sites were characterized by high Cu concentrations, whereas park sites were associated with a higher presence of Mg.

PC2 was not included in the analysis, as the projection of the cases on this factor did not generate a clear output within the context of this case study. As shown by the PC projections on original variables shown in SM2, PC2 was mostly driven by Ti, whose concentration were found to be poorly correlated with the sources, as indicated previously in Section 3.2.

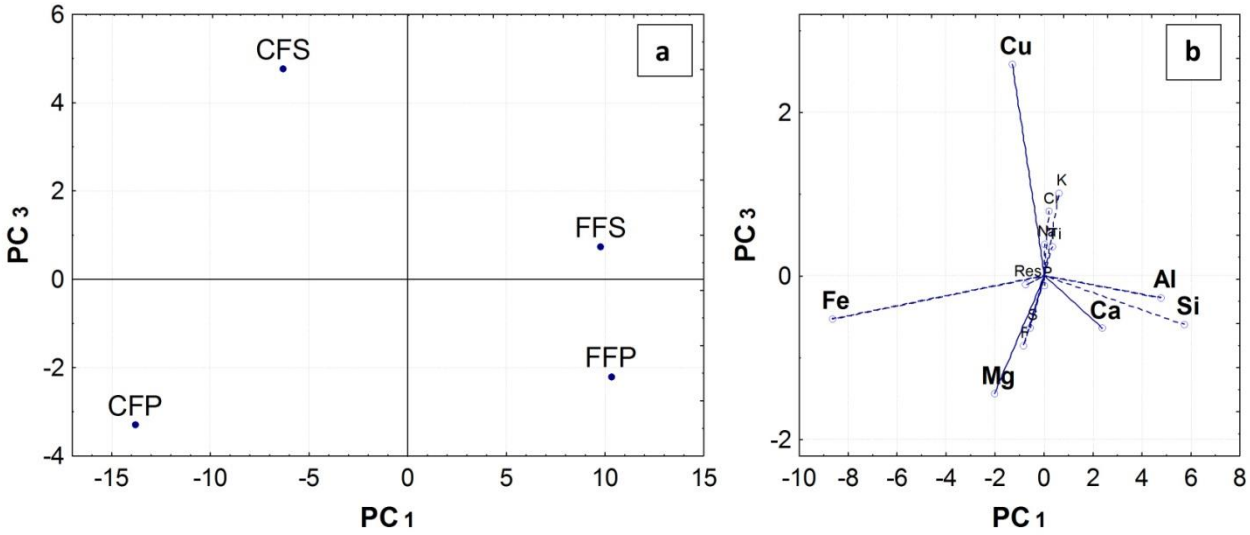

Figure 6 – Principal component analysis: (a) model representation of sampling sites separation; (b) relative variable loadings.

3.4 Quantitative and qualitative data comparison

The data acquired from EDX analysis were finally used to assess the quality of PM at the sampling sites and their differential effect on the accumulation of elements. $W_{\%}$ values were combined with quantitative data of PM deposition on leaf area basis calculated from the filter weights (Sgrigna et al. 2015). The assessment identified key elements as polluting markers: Fe for steel factory and Cu for road traffic. Table 3 presents the estimates of Fe and Cu removed per leaf area unit (mg m^{-2}) at the four sites, which were obtained as the product of $W_{\%}$ and the quantitative data resulting by weighing the same filters analyzed through SEM/EDX (Table SM3). The highest values of removal for Fe and Cu were found close to the factory, at the park (CFP) and street (CFS) sites, respectively.

Table. 3 – Upscaling of Fe and Cu concentrations on leaf area basis in the four sampling sites.

mg m^{-2}	**FFP**	**FFS**	**CFP**	**CFS**

Fe	2.7 ± 0.7	2.6 ± 0.6	8.4± 2.0	6.7 ± 1.5
Cu	0.005 ± 0.001	0.019 ± 0.004	0.19 ± 0.5	2.6 ± 0.8

4. Discussion

The mean particle diameter values separately obtained by the SEM analysis from the four sampling sites were almost homogeneous, and the mean particle diameter determined on the whole sampling set (1.57 ± 0.06 μm) was in line with typical dust particle size in an urban environment (Blanco et al., 2003; Ondráček et al., 2011). However, analyzing the particle size distribution through lognormal functions, multi-modal fitting procedures revealed significant differences between the sites. In particular, three particle size families were identified, whose relative abundance changed between the sites and with distance from the ground. These particle families were associated with three fitting modes, labeled “Background,” “Street,” and “Factory,” with their distributions centered at about 1.2, 2.6, and 0.6 μm, respectively.

Our aforementioned particle classification corroborates with Pugatshova et al. (2007), belonging to the following two typical groups of PM from urban environments: the accumulation range (between 0.1 and 1 μm) and mechanical aerosols (>1 μm). The latter class is also defined as “coarse particles.” Morawska et al.(Morawska et al., 2008) distinguished such particle classes also based on their origin: fine particles (PM < 1 μm) are linked to anthropogenic sources that involve high-temperature processes, although minor contributions from mechanical material abrasion cannot be negated; coarse particles (PM > 1 μm) are mostly generated by mechanical actions such as material abrasion and/or dust resuspension, and are largely associated with anthropogenic activities.

The 1.2-μm peak (“Background”) describes the most important group of particles. The distributions reported in Figure 3 demonstrate that “Background” particles are included in both the “accumulation” (< 1 μm) and “coarse” (> 1 μm) range. This group is reasonably describing a family of particles generated by multiple

sources, most likely including the contributions from the streets and the nearby factory. In addition, the presence of larger particles (> 1 µm) together with the typical accumulation range group could be due to the transient temporal shift in their size range, mainly attributed to particle coagulation up until deposition on the leaf surfaces. It is noteworthy that the particles analyzed in this study pertain to accumulated dust on leaves, and are not directly acquired from ambient atmospheric measurements. The large amount of coarse particles in our samples (acquired from the leaf wash off) also contribute to the lifetime of this size class, which is considered as the more persistent group of particles among all the PM classes (Willeke and Whitby, 1975). Further, due consideration should be given to the possible particle aggregation that might have occurred during the solution phase (Hofman et al.(2014b).

The mode centered at around 2.6 µm (Street) essentially comprised coarse particles, and was mainly attributed to traffic sources following interpretation from previous research linking the coarse fraction to tyre wear, road abrasion, and re-suspended dust (Harrison et al., 2012; Lenschow et al., 2010; Ondráček et al., 2011; Pant and Harrison, 2013; Thorpe and Harrison, 2008). The relative abundance of such particles in the lower part of tree crown depicts the availability of their source at the ground level, which could be either through direct emission or particle resuspension. Moreover, their mean weight (due both to their size and elemental composition) inhibits rapid particle diffusion at higher crown levels. However, abundance of coarse particles in the lower crown could be also related to their removal from the upper crown under meteorological influences (Przybysz et al., 2014; Willeke and Whitby, 1975).

The mode centered at 0.6 µm, mainly representing the particles in the accumulation range, has been associated to factory-derived PM. This is consistent to a previous study conducted in the city of Shanghai (China), which also noted a mode centered at 0.6 µm, characterized by a large steel industrial district while analyzing the PM size distribution from three different urban sites (suburban, urban, and industrial) using lognormal curve fitting (Waheed et al., 2011). Therefore, we can suggest considering this peak as a fingerprint of the PM associated with steel factory. Similar abundance (*A*) at any crown height, for both the sampled trees close to the factory (CFP and CFS), suggests a homogeneous diffusion capability of the “Factory” mode

particles. On the other hand, the lower relative abundance registered at the lower crown level of street tree indicate the limitations of “Street” mode particles.

The differences evidenced by particle size distribution analysis between the sampling sites have been substantiated through elemental analysis. This is particularly evident when associating Fe concentration to the steel factory, from both the weighted volume percentage analysis (Figure 5) and PCA results (Figure 6). However, several studies have also identified Fe having origins from traffic sources (Adamo et al., 2008; Amato et al., 2009; Ault et al., 2012; Catinon et al., 2013; Maher et al., 2008), and somehow the comparison between samples from FFP and FFS sites also describes this trend (a higher Fe concentration is recorded at FFS site). However, the traffic-related effect on Fe concentration is dwarfed by the overwhelming factory influence, which increases the average Fe concentration by a factor of three. Other factory fingerprints are all the residual metal elements (except for Zn), namely Cr, Ni, Mo, Sn, Sb, Ba, W, and Bi, which were found at higher levels in the factory area.

The main traffic-related marker evidenced by the EDX analysis, and confirmed by the PCA in this study is Cu, which is reportedly generated by mechanical abrasion of car components, particularly tyre wear breakdown (Pant and Harrison, 2013) or brake wear (Grigoratos and Martini, 2015). The high Cu concentration found at the site close to both the factory and street (CFS) can be due to the presence of a busy road with a little slope in the proximity of a roundabout. In previous studies, these conditions have been associated with a quick decrease of the speed of cars, thereby enhancing the presence of traffic-related particles (Wilkinson et al., 2013). Moreover, our $W_{\%}$ data indicates higher concentrations of Cu, Cr and Cl near street sites, which is consistent to previous studies (Gietl et al., 2010; Ondráček et al., 2011; Stechmann and Dannecker, 1990; Thorpe and Harrison, 2008), however, this was not confirmed by PCA. On the other hand, PCA evidenced Mg as a non-traffic marker, corroborating with a previous study which recognized it as an element related to particles from natural sources (Senlin et al., 2008). The random occurrence of Ti, in terms of location- and source-dependence is noteworthy, and this aspect requires further investigation. Previous studies have recognized it as a typical component of urban particles (Stechmann and Dannecker, 1990), and also associated with pavement resuspension (Amato et al., 2009; Jancsek-Turóczi et al., 2013).

As this study presents a protocol for characterizing PM from the dimensional and chemical points of view, we would like to highlight the added value to use PM deposited on urban trees for such a study. The magnitude of Fe and Cu deposition that we show here on leaf area basis are not only an interesting tool to parameterize the air quality of different areas, but also an important input for those modelers who aim at studying air pollution mitigation by urban trees (Escobedo et al., 2011), including the implications for their physiological adaptation (Calfapietra et al., 2015). Moreover, the specific qualitative–quantitative data of PM deposited on trees in populated areas serve as an evidence base for strategic urban green management to maximize air pollution removal by trees. The case study presented here was conducted through a combination of relatively simple and low-cost techniques. The same methodology could be applied to several different cities and their peculiar tree species. This is being realized in the context of the COST Action FP1204 GreenInUrbs (www.greeninurbs.com) involving several European cities, aiming to provide a useful tool for low-cost, diffused monitoring of PM pollutant and their management by urban forests across Europe.

5. Conclusions

Our study demonstrated the potential of urban tree leaves as cost-effective passive air samplers for diffused monitoring and characterization of PM pollutants in distinct urban environments. The combination of SEM/EDX analysis along with the mathematical elaborations applied to the case study show the merit of utilizing tree leaves in acquiring additional information on source-characterized PM quality across the studied area, not conceivable otherwise by the mere mean particle size analysis. Our approach allowed distinguishing the sampling sites based on both the particle size distribution and their elemental composition through application of lognormal multi-modal fitting and PCA, respectively. Tree location was identified as a key strategic factor in utilizing them as air pollutant sinks within the urban environments. Upscaling these results on leaf area basis provided a useful indicator for strategic evaluation of specific harmful PM pollutants using trees across a city. Future studies based on this methodology on a larger number of samples can provide a finer distinction of PM quality in order to identify more diverse urban sources.

Our study is pertinent to urban planners and other stakeholders in the context of sustainable mitigation of the harmful health effects of PM in the urban environment, particularly calling for a more strategic role of urban trees in robust air quality monitoring and management on a routine basis.

6. Acknowledgements

This study was inspired within the framework of the COST FP1204 “GreenInUrbs” project. The research activities were carried out as part of the RIFORTER project “Studio di RIqualificazione della FOResta urbana per il miglioramento della qualita dell'aria della conca ternana”, funded by Fondazione CARIT. We acknowledge project PON Infrastructure Amica (High Technology Infrastructure for Climate and Environment Monitoring PONa3_00363) for the availability of the SEM-EDX facility, and the MIUR-PRIN 2012 project “NEUFOR” for funding travels during the experiments. This study was also supported by NPU I program (LO1415). Special thanks are also due to the contribution of Luca Leonardi (IBAF–CNR associated), Christopher Mollica, and Claudia Tarmanti (IBAF – CNR collaborators).

7. References

Ackermann, I.J., Hass, H., Memmesheimer, M., Ebel, a., Binkowski, F.S., Shankar, U., 1998. Modal aerosol dynamics model for Europe development and first applications. Atmos. Environ. 32, 2981–2999. doi:10.1016/S1352-2310(98)00006-5

Adamo, P., Giordano, S., Naimo, D., Bargagli, R., 2008. Geochemical properties of airborne particulate matter (PM10) collected by automatic device and biomonitors in a Mediterranean urban environment. Atmos. Environ. 42, 346–357. doi:10.1016/j.atmosenv.2007.09.018

Amato, F., Pandolfi, M., Viana, M., Querol, X., Alastuey, a., Moreno, T., 2009. Spatial and chemical patterns of PM10 in road dust deposited in urban environment. Atmos. Environ. 43, 1650–1659. doi:10.1016/j.atmosenv.2008.12.009

Anderson, J.O., Thundiyil, J.G., Stolbach, A., 2012. Clearing the Air: A Review of the Effects of Particulate Matter Air Pollution on Human Health. J. Med. Toxicol. 8, 166–175. doi:10.1007/s13181-011-0203-1

Apopa, P.L., Qian, Y., Shao, R., Guo, N.L., Schwegler-Berry, D., Pacurari, M., Porter, D., Shi, X., Vallyathan, V., Castranova, V., Flynn, D.C., 2009. Iron oxide nanoparticles induce human microvascular endothelial

cell permeability through reactive oxygen species production and microtubule remodeling. Part. Fibre Toxicol. 6, 1. doi:10.1186/1743-8977-6-1

Ault, A.P., Peters, T.M., Sawvel, E.J., Casuccio, G.S., Willis, R.D., Norris, G. a., Grassian, V.H., 2012. Single-particle SEM-EDX analysis of iron-containing coarse particulate matter in an urban environment: Sources and distribution of iron within Cleveland, Ohio. Environ. Sci. Technol. 46, 4331–4339. doi:10.1021/es204006k

Beckett, K.P., Freer-Smith, P.H., Taylor, G., 1998. Urban woodlands: their role in reducing the effects of particulate pollution. Environ. Pollut. 99, 347–60.

Blanco, a., de Tomasi, F., Filippo, E., Manno, D., Perrone, M.R., Serra, R., Tafuro, a. M., Tepore, a., 2003. Characterization of African dust over southern Italy. Atmos. Chem. Phys. Discuss. 3, 4633–4670. doi:10.5194/acpd-3-4633-2003

Calfapietra, C., Fares, S., Manes, F., Morani, a, Sgrigna, G., Loreto, F., 2013. Role of Biogenic Volatile Organic Compounds (BVOC) emitted by urban trees on ozone concentration in cities: a review. Environ. Pollut. 183, 71–80. doi:10.1016/j.envpol.2013.03.012

Calfapietra, C., Peñuelas, J., Niinemets, Ü., 2015. Urban plant physiology: adaptation-mitigation strategies under permanent stress. Trends Plant Sci. 20, 72–75. doi:10.1016/j.tplants.2014.11.001

Capelli, L., Sironi, S., Del Rosso, R., Céntola, P., Rossi, A., Austeri, C., 2011. Olfactometric approach for the evaluation of citizens' exposure to industrial emissions in the city of Terni, Italy. Sci. Total Environ. 409, 595–603. doi:10.1016/j.scitotenv.2010.10.054

Catinon, M., Ayrault, S., Boudouma, O., Bordier, L., Agnello, G., Reynaud, S., Tissut, M., 2013. Are coarse particles unexpected common reservoirs for some atmospheric anthropogenic trace elements? A case study. Atmos. Environ. 74, 217–226. doi:10.1016/j.atmosenv.2013.03.059

Cattuto, C., Gregori, L., Melelli, L., Taramelli, a., Troiani, C., 2002. Paleogeographic evolution of the Terni basin (Umbria, Italy). Boll. Soc. Ital. 1, 865–872.

Cheng, Z., Jiang, J., Fajardo, O., Wang, S., Hao, J., 2013. Characteristics and health impacts of particulate matter pollution in China (2001-2011). Atmos. Environ. 65, 186–194. doi:10.1016/j.atmosenv.2012.10.022

Dai, L., Zanobetti, A., Koutrakis, P., Schwartz, J.D., 2014. Associations of fine particulate matter species with mortality in the united states: A multicity time-series analysis. Environ. Health Perspect. 122, 837–842. doi:10.1289/ehp.1307568

Deshmukh, D.K., Deb, M.K., Verma, D., Verma, S.K., Nirmalkar, J., 2012. Aerosol size distribution and seasonal variation in an urban area of an industrial city in central India. Bull. Environ. Contam. Toxicol. 89, 1098–1104. doi:10.1007/s00128-012-0834-1

Dockery, D.W., Pope, A.C., Xu, X., Spengler, J.D., Ware, J.H., Fay, M.E., Ferris, B., Speizer, F.E., 1993. An association between air pollution and mortality in six U.S. cities. N. Engl. J. Med. 329.

Donaldson, K., Seaton, A., 2012. A short history of the toxicology of inhaled particles. Part. Fibre Toxicol. 9, 13. doi:10.1186/1743-8977-9-13

Dzierzanowski, K., Popek, R., Gawrońska, H., Saebø, A., Gawroński, S.W., 2011. Deposition of particulate matter of different size fractions on leaf surfaces and in waxes of urban forest species. Int. J. Phytoremediation 13, 1037–46. doi:10.1080/15226514.2011.552929

Escobedo, F.J., Kroeger, T., Wagner, J.E., 2011. Urban forests and pollution mitigation: analyzing ecosystem services and disservices. Environ. Pollut. 159, 2078–87. doi:10.1016/j.envpol.2011.01.010

Freer-Smith, P.H., Beckett, K.P., Taylor, G., 2005. Deposition velocities to Sorbus aria, Acer campestre, Populus deltoides X trichocarpa "Beaupré", Pinus nigra and X Cupressocyparis leylandii for coarse, fine and ultra-fine particles in the urban environment. Environ. Pollut. 133, 157–67. doi:10.1016/j.envpol.2004.03.031

Gietl, J.K., Lawrence, R., Thorpe, A.J., Harrison, R.M., 2010. Identification of brake wear particles and derivation of a quantitative tracer for brake dust at a major road. Atmos. Environ. 44, 141–146. doi:10.1016/j.atmosenv.2009.10.016

Grigoratos, T., Martini, G., 2015. Brake wear particle emissions: a review. Environ. Sci. Pollut. Res. 22, 2491–2504. doi:10.1007/s11356-014-3696-8

Harrison, R.M., Jones, A.M., Gietl, J., Yin, J., Green, D.C., 2012. Estimation of the contributions of brake dust, tire wear, and resuspension to nonexhaust traffic particles derived from atmospheric measurements. Environ. Sci. Technol. 46, 6523–6529. doi:10.1021/es300894r

Hofman, J., Lefebvre, W., Janssen, S., Nackaerts, R., Nuyts, S., Mattheyses, L., Samson, R., 2014a. Increasing the spatial resolution of air quality assessments in urban areas: A comparison of biomagnetic monitoring and urban scale modelling. Atmos. Environ. 92, 130–140. doi:10.1016/j.atmosenv.2014.04.013

Hofman, J., Wuyts, K., Van Wittenberghe, S., Brackx, M., Samson, R., 2014b. Reprint of On the link between biomagnetic monitoring and leaf-deposited dust load of urban trees: relationships and spatial variability of different particle size fractions. Environ. Pollut. 192, 285–94. doi:10.1016/j.envpol.2014.05.006

Jancsek-Turóczi, B., Hoffer, A., Nyírő-Kósa, I., Gelencsér, A., 2013. Sampling and characterization of resuspended and respirable road dust. J. Aerosol Sci. 65, 69–76. doi:10.1016/j.jaerosci.2013.07.006

Janhäll, S., Andreae, M.O., Pöschl, U., 2009. Biomass burning aerosol emissions from vegetation fires: particle number and mass emission factors and size distributions. Atmos. Chem. Phys. Discuss. 9, 17183–17217. doi:10.5194/acpd-9-17183-2009

Jin, S., Guo, J., Wheeler, S., Kan, L., Che, S., 2014. Evaluation of impacts of trees on PM2.5 dispersion in urban streets. Atmos. Environ. 99, 277–287. doi:10.1016/j.atmosenv.2014.10.002

Kariisa, M., Foraker, R., Pennell, M., Buckley, T., Diaz, P., Criner, G.J., Wilkins, J.R., 2014. Short- and Long-Term Effects of Ambient Ozone and Fine Particulate Matter on the Respiratory Health of Chronic Obstructive Pulmonary Disease Subjects. Arch. Environ. Occup. Health 70, 56–62. doi:10.1080/19338244.2014.932753

Kumar, P., Gurjar, B.R., Nagpure, a. S., Harrison, R.M., 2011. Preliminary estimates of nanoparticle number emissions from road vehicles in megacity Delhi and associated health impacts. Environ. Sci. Technol. 45, 5514–5521. doi:10.1021/es2003183

Lee, K.W., Chen, H., 1984. Coagulation Rate of Polydisperse Particles. Aerosol Sci. Technol. 3, 327–334. doi:10.1080/02786828408959020

Lenschow, P., Abraham, H., Kutzner, K., Lutz, M., Preub, J., Reichenbficher, W., 2010. ENVIRONMENT Some ideas about the sources of PM10 0, 23–33.

Llausàs, A., Roe, M., 2012. Green Infrastructure Planning: Cross-National Analysis between the North East of England (UK) and Catalonia (Spain). Eur. Plan. Stud. 20, 641–663. doi:10.1080/09654313.2012.665032

Lorenzini, G., Grassi, C., Nali, C., Petiti, a., Loppi, S., Tognotti, L., 2006. Leaves of Pittosporum tobira as indicators of airborne trace element and PM10 distribution in central Italy. Atmos. Environ. 40, 4025–4036. doi:10.1016/j.atmosenv.2006.03.032

Lu, S., Liu, D., Zhang, W., Liu, P., Fei, Y., Gu, Y., Wu, M., Yu, S., Yonemochi, S., Wang, X., Wang, Q., 2015. Physico-chemical characterization of PM2.5 in the microenvironment of Shanghai subway. Atmos. Res. 153, 543–552. doi:10.1016/j.atmosres.2014.10.006

Lu, S.G., Zheng, Y.W., Bai, S.Q., 2008. A HRTEM/EDX approach to identification of the source of dust particles on urban tree leaves. Atmos. Environ. 42, 6431–6441. doi:10.1016/j.atmosenv.2008.04.039

Maher, B. a., Moore, C., Matzka, J., 2008. Spatial variation in vehicle-derived metal pollution identified by magnetic and elemental analysis of roadside tree leaves. Atmos. Environ. 42, 364–373. doi:10.1016/j.atmosenv.2007.09.013

McDonald, a. G., Bealey, W.J., Fowler, D., Dragosits, U., Skiba, U., Smith, R.I., Donovan, R.G., Brett, H.E., Hewitt, C.N., Nemitz, E., 2007. Quantifying the effect of urban tree planting on concentrations and depositions of PM10 in two UK conurbations. Atmos. Environ. 41, 8455–8467. doi:10.1016/j.atmosenv.2007.07.025

Merkus, H.G., 2009. Particle Size Measurements, Springer S. ed, Particle Technology.

Morani, A., Nowak, D.J., Hirabayashi, S., Calfapietra, C., 2011. How to select the best tree planting locations to enhance air pollution removal in the MillionTreesNYC initiative. Environ. Pollut. 159, 1040–7. doi:10.1016/j.envpol.2010.11.022

Morawska, L., Keogh, D.U., Thomas, S.B., Mengersen, K., 2008. Modality in ambient particle size distributions and its potential as a basis for developing air quality regulation. Atmos. Environ. 42, 1617–1628. doi:10.1016/j.atmosenv.2007.09.076

Nowak, D.J., Crane, D.E., Stevens, J.C., Hoehn, R.E., Walton, J.T., 2008. A Ground-Based Method of Assessing Urban Forest Structure and Ecosystem Services 34, 347–358.

Ondráček, J., Schwarz, J., Ždímal, V., Andělová, L., Vodička, P., Bízek, V., Tsai, C.J., Chen, S.C., Smolík, J., 2011. Contribution of the road traffic to air pollution in the Prague city (busy speedway and suburban crossroads). Atmos. Environ. 45, 5090–5100. doi:10.1016/j.atmosenv.2011.06.036

Pant, P., Harrison, R.M., 2013. Estimation of the contribution of road traffic emissions to particulate matter concentrations from field measurements: A review. Atmos. Environ. 77, 78–97. doi:10.1016/j.atmosenv.2013.04.028

Paoletti, L., De Berardis, B., Arrizza, L., Passacantando, M., Inglessis, M., Mosca, M., 2003. Seasonal effects on the physico-chemical characteristics of PM2.1 in Rome: A study by SEM and XPS. Atmos. Environ. 37, 4869–4879. doi:10.1016/j.atmosenv.2003.08.031

Peachey, C.J., Sinnett, D., Wilkinson, M., Morgan, G.W., Freer-Smith, P.H., Hutchings, T.R., 2009. Deposition and solubility of airborne metals to four plant species grown at varying distances from two heavily trafficked roads in London. Environ. Pollut. 157, 2291–9. doi:10.1016/j.envpol.2009.03.032

Popek, R., Gawrońska, H., Wrochna, M., Gawroński, S.W., Sæbø, A., 2013. Particulate Matter on Foliage of 13 Woody Species: Deposition on Surfaces and Phytostabilisation in Waxes – a 3-Year Study. Int. J. Phytoremediation 15, 245–256. doi:10.1080/15226514.2012.694498

Przybysz, a., Sæbø, a., Hanslin, H.M., Gawroński, S.W., 2014. Accumulation of particulate matter and trace elements on vegetation as affected by pollution level, rainfall and the passage of time. Sci. Total Environ. 481, 360–369. doi:10.1016/j.scitotenv.2014.02.072

Pugatshova, A., Reinart, A., Tamm, E., 2007. Features of the multimodal aerosol size distribution depending on the air mass origin in the Baltic region. Atmos. Environ. 41, 4408–4422. doi:10.1016/j.atmosenv.2007.01.044

Querol, X., Moreno, T., Karanasiou, a., Reche, C., Alastuey, a., Viana, M., Font, O., Gil, J., De Miguel, E., Capdevila, M., 2012. Variability of levels and composition of PM 10 and PM 2.5 in the Barcelona metro system. Atmos. Chem. Phys. 12, 5055–5076. doi:10.5194/acp-12-5055-2012

Samet, J.M., Dominici, F., Curriero, F.C.., Coursac, I., 2000. Fine particulate air pollution and mortality in 20 U.S. cities. N. Engl. J. Med. 343, 1742 – 1749. doi:10.1056/NEJM199902183400701

Sawidis, T., Breuste, J., Mitrovic, M., Pavlovic, P., Tsigaridas, K., 2011. Trees as bioindicator of heavy metal pollution in three European cities. Environ. Pollut. 159, 3560–70. doi:10.1016/j.envpol.2011.08.008

Senlin, L., Zhenkun, Y., Xiaohui, C., Minghong, W., Guoying, S., Jiamo, F., Paul, D., 2008. The relationship between physicochemical characterization and the potential toxicity of fine particulates (PM2.5) in Shanghai atmosphere. Atmos. Environ. 42, 7205–7214. doi:10.1016/j.atmosenv.2008.07.030

Sgrigna, G., Sæbø, a., Gawronski, S., Popek, R., Calfapietra, C., 2015. Particulate Matter deposition on Quercus ilex leaves in an industrial city of central Italy. Environ. Pollut. 197, 187–194. doi:10.1016/j.envpol.2014.11.030

Simon, E., Baranyai, E., Braun, M., Cserháti, C., Fábián, I., Tóthmérész, B., 2014. Elemental concentrations in deposited dust on leaves along an urbanization gradient. Sci. Total Environ. 490, 514–20. doi:10.1016/j.scitotenv.2014.05.028

Smith, M.H., Park, P.M., Consterdine, I.E., 1993. Marine aerosol concentrations and estimated fluxes over the sea. Quart. J. Roy. Meteor. Soc. 119, 809–824. doi:10.1002/qj.49711951211

Söderlund, J., Kiss, L., Niklasson, G., Granqvist, C., 1998. Lognormal Size Distributions in Particle Growth Processes without Coagulation. Phys. Rev. Lett. 80, 2386–2388. doi:10.1103/PhysRevLett.80.2386

Song, Y., Maher, B. a., Li, F., Wang, X., Sun, X., Zhang, H., 2015. Particulate matter deposited on leaf of five evergreen species in Beijing, China: Source identification and size distribution. Atmos. Environ. 105, 53–60. doi:10.1016/j.atmosenv.2015.01.032

Stechmann, H., Dannecker, W., 1990. Characterization and source analysis of vehicle-generated aerosols. J. Aerosol Sci. 21, S287–S290. doi:10.1016/0021-8502(90)90240-X

Tadmor, J., 1971. Consideration of deposition of pollutants in the design of a stack height. Atmos. Environ. 5, 473–482.

Thorpe, A., Harrison, R.M., 2008. Sources and properties of non-exhaust particulate matter from road traffic: A review. Sci. Total Environ. 400, 270–282. doi:10.1016/j.scitotenv.2008.06.007

Tiwary, A., Morvan, H.P., Colls, J.J., 2006. Modelling the size-dependent collection efficiency of hedgerows for ambient aerosols. J. Aerosol Sci. 37, 990–1015. doi:10.1016/j.jaerosci.2005.07.004

Tiwary, A., Sinnett, D., Peachey, C., Chalabi, Z., Vardoulakis, S., Fletcher, T., Leonardi, G., Grundy, C., Azapagic, A., Hutchings, T.R., 2009. An integrated tool to assess the role of new planting in PM10 capture and the human health benefits: a case study in London. Environ. Pollut. 157, 2645–53. doi:10.1016/j.envpol.2009.05.005

Tomašević, M., Vukmirović, Z., Rajšić, S., Tasić, M., Stevanović, B., 2005. Characterization of trace metal particles deposited on some deciduous tree leaves in an urban area. Chemosphere 61, 753–760. doi:10.1016/j.chemosphere.2005.03.077

Viana, M., Kuhlbusch, T. a. J., Querol, X., Alastuey, a., Harrison, R.M., Hopke, P.K., Winiwarter, W., Vallius, M., Szidat, S., Prévôt, a. S.H., Hueglin, C., Bloemen, H., Wåhlin, P., Vecchi, R., Miranda, a. I., Kasper-Giebl, a., Maenhaut, W., Hitzenberger, R., 2008. Source apportionment of particulate matter in Europe: A review of methods and results. J. Aerosol Sci. 39, 827–849. doi:10.1016/j.jaerosci.2008.05.007

Waheed, A., Li, X., Tan, M., Bao, L., Liu, J., Zhang, Y., Zhang, G., Li, Y., 2011. Size Distribution and Sources of Trace Metals in Ultrafine/Fine/Coarse Airborne Particles in the Atmosphere of Shanghai. Aerosol Sci. Technol. 45, 163–171. doi:10.1080/02786826.2010.528079

Warheit, D.B., Webb, T.R., Colvin, V.L., Reed, K.L., Sayes, C.M., 2007. Pulmonary bioassay studies with nanoscale and fine-quartz particles in rats: Toxicity is not dependent upon particle size but on surface characteristics. Toxicol. Sci. 95, 270–280. doi:10.1093/toxsci/kfl128

Wilkinson, K.E., Lundkvist, J., Netrval, J., Eriksson, M., Seisenbaeva, G. a., Kessler, V.G., 2013. Space and time resolved monitoring of airborne particulate matter in proximity of a traffic roundabout in Sweden. Environ. Pollut. 182, 364–370. doi:10.1016/j.envpol.2013.07.043

Willeke, K., Whitby, K.T., 1975. Atmospheric Aerosols: Size Distribution Interpretation. J. Air Pollut. Control Assoc. 25, 529–534. doi:10.1080/00022470.1975.10470110

William C. Hinds, 1999. Aerosol technology. J. Aerosol Sci. 14, 175. doi:10.1016/0021-8502(83)90049-6